

# Current Drive Enhancement of Strained Ge nMISFET with SiGe Stressors by Uniaxial Tensile Stress

Yuuichi Kamimuta, Yoshihiko Moriyama, Keiji Ikeda, Minoru Oda, and Tsutomu Tezuka

MIRAI-Toshiba

1 Komukai Toshiba-cho, Saiwai-ku, Kawasaki, 212-8582, Japan

Phone: +81-44-549-2314 E-mail: yuuichi.kamimuta@toshiba.co.jp

## 1. Introduction

Ge channel MISFETs have been proposed as a promising candidate of future device structures over the scaling limit of Si technology, because of the higher carrier mobility than Si (two times for electrons and four times for holes). Channel strain engineering is currently very successful in Si MISFETs in terms of the enhancement of carrier mobility and transistor performance. It has been theoretically reported [1] that electron mobility enhancement of Ge channel by introducing uniaxial strain. Moreover, the effect of the tensile strain on Ge nMISFET performance was also reported by using bending apparatus [2] [3]. These result concluded that the uniaxial tensile strain enhanced the electron mobility of Ge nMISFETs, similar to Si nMISFETs. Most desirable approach to introduce uniaxial tensile strain in the Ge channel is through the integration of SiGe source and drain (S/D) with a smaller lattice constant than Ge. SiGe S/D can be easily integrated in Ge nMISFETs [4], similar to the integration of Si:C S/D in Si nMISFETs [5]. In addition, higher strain is induced in the channel with a smaller gate length ( $L_g$ ) with SiGe stressor.

In this paper, we investigate the current drive enhancement of strained Ge nMISFET introducing uniaxial tensile strain by employing SiGe S/D stressor for the first time.

## 2. Experimental

The device fabrication flow is shown in **Fig. 1**. The substrates used in this study were pGe (001) ( $\sim 0.1\Omega\text{cm}$ ). After device isolation, 6nm thick CVD-SiO<sub>2</sub> was deposited as a gate dielectric after deposition of 7ML Si passivation layer [6] without implantation of channel impurity ions. TaN and a-Si were sputtered as a gate electrode. The gate patterning was done by E-beam lithography process with a SiO<sub>2</sub> hard mask. After SiO<sub>2</sub> sidewall formation, recess structures were etched by wet solution. Next, SiGe Selective Epitaxial Growth (SEG) was applied on the recess regions. The Ge composition,  $x$ , of SiGe stressor was 0.7, 0.8 and 1.0 (Ge) [7]. During SEG, hardmask and sidewalls covered metal gate. P<sup>+</sup> implantation was carried out to the S/D regions. After activation anneal (500°C), BEOL process was performed at the maximum temperature of 420°C. On the control wafer, the Ge recess etching and SEG were not performed. The strain applied in Ge channel layers was measured with micro-Raman spectroscopy by using the SiO<sub>2</sub> dummy gate samples [7].

## 3. Results and Discussion

**Fig. 2** shows cross-sectional transmission electron microscopy (TEM) images of the nMISFET after SiGe ( $x = 0.7$ ) SEG. 50nm-thick embedded SiGe stressor was clearly observed. From this image, it is also confirmed that sidewall length ( $L_{sw}$ ) is about 25nm.

**Fig. 3** shows ( $L_g + 2L_{sw}$ ) dependence of average uniaxial tensile strain in Ge channel regions with the SiGe stressors. These values were estimated from the Raman peak shifts for the Ge-Ge vibration mode, according to the manner published in [8] [9]. It is confirmed that the values of uniaxial tensile strain increase with decreasing ( $L_g + 2L_{sw}$ ), and  $x$  of SiGe stressors. The tendency is consistent with that for

Si-MOSFETs with Si:C stressors [10].

I-V curves of n<sup>+</sup>Ge/pGe and n<sup>+</sup>SiGe/pSiGe diodes are shown in **Fig. 4**. These diodes exhibit rectifying characteristics over the range of  $x$  of the SiGe stressor. The reverse current is, however, becomes higher for lower  $x$ . This result may be attributed to defects near the SiGe/Ge interface.

**Fig. 5** and **Fig. 6** show  $I_s$ - $V_g$  characteristics for nMISFET with SiGe ( $x = 0.7$ ) stressor. In  $L_g = 1\mu\text{m}$  device,  $I_{ON}/I_{OFF}$  ratio of 3 orders of magnitude was obtained. Although  $I_{ON}/I_{OFF}$  ratio and Subthreshold Slope (SS) were significantly degraded for shorter  $L_g$  devices due to the thick EOT and the low channel-impurity concentration, FET operation has been observed down to 50nm  $L_g$  as shown in **Fig. 6**.

In order to estimate the effect of local tensile strain on the current drive, the maximum transconductance ( $G_{m,max}$ ) was extracted as a function of  $L_g$ . **Fig. 7** compares the  $L_g$  dependence of the normalized  $G_{m,max}$  in the linear regime, which is defined as  $G_{m,max}(L_g) / G_{m,max}(L_g = 1\mu\text{m})$ . It was found that the enhancement factor of the normalized  $G_{m,max}$  against the control devices was increased for shorter  $L_g$  devices and was amounted to be 1.3 and 1.6 at  $L_g = 50\text{nm}$  for  $x = 0.8$  and  $x = 0.7$ , respectively. Electron mobility enhancement factors of 1.6 and 2 against an unstrained (001) Ge nMISFET are estimated [1] from the measured uniaxial tensile strain values of 0.4% and 0.6% for  $x = 0.8$  and  $x = 0.7$  devices at  $L_g = 50\text{nm}$  (i.e.  $L_g + 2L_{sw} = 100\text{nm}$ ), respectively, as shown in **Fig. 3**. The obtained linear  $G_{m,max}$  enhancements are reasonable considering the mobility enhancement factors. The deviation may be due to high parasitic S/D resistance of the present devices. In the saturation regime, the enhancement factor of the normalized  $G_{m,max}$  was decreased (**Fig. 8**) but the values were almost consistent with a relation of  $I_{dsat} \propto \mu^{0.5}$  [11] [12] as shown **Fig. 9**. The result suggest that the current drive enhancement for short channel devices is originated from the tensile strain in the Ge channel adjacent to the SiGe S/D stressors.

## 4. Conclusions

Fabrication of the strained Ge nMISFETs having SiGe S/D stressors with  $L_g$  down to 50nm and the strain-induced current drivability enhancement were successfully demonstrated. The  $G_{m,max}$  enhancement factor of strained SiGe S/D nMISFETs was found to be consistent with the measured strain dependences on  $L_g$  and  $x$  in SiGe S/D. These results suggest that uniaxial tensile strain generated by SiGe S/D stressors is effective for the performance booster of scaled Ge nMISFET.

## Acknowledgements

The authors are grateful to Dr. T. Horikawa and technical staff in AIST-NIRC for their support in the sample fabrication. This work was supported by NEDO.

**References**

[1] Y. J. Yang et al., *Appl. Phys. Lett.*, **91**(10) 102103 (2007).  
 [2] M. Kobayashi et al., *IEEE Trans. Electron Devices*, **57**(5) 1037 (2010).  
 [3] Y.-C. Fu et al., *IEDM Tech. Dig.*, 2010, 432.  
 [4] G. L. Luo et al., *IEDM Tech. Dig.*, 2009, 689.  
 [5] K. W. Ang et al., *IEDM Tech. Dig.*, 2004, 1069.  
 [6] N. Taoka et al., *Jpn. J. Appl. Phys.*, **49** 04DA09 (2010).  
 [7] Y. Moriyama et al., *Solid State Electron.*, **60** 89(2011).  
 [8] T. Ito et al., *Jpn. J. Appl. Phys.* **33** 171 (1994).  
 [9] J. C. Tsang et al., *J. Appl. Phys.* **75** 8098 (1994).  
 [10] M. Bauer et al., *ECS Transactions* **16**(10) 1001(2008).  
 [11] R. Ohba et al., *IEEE Trans. Electron Devices*, **48** 338 (2001).  
 [12] K. Tatsumura et al., *IEDM Tech. Dig.*, 2009, 465.

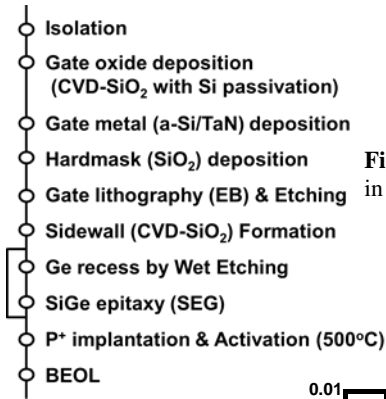


**Fig. 1** Process flow employed in MISFET fabrication.

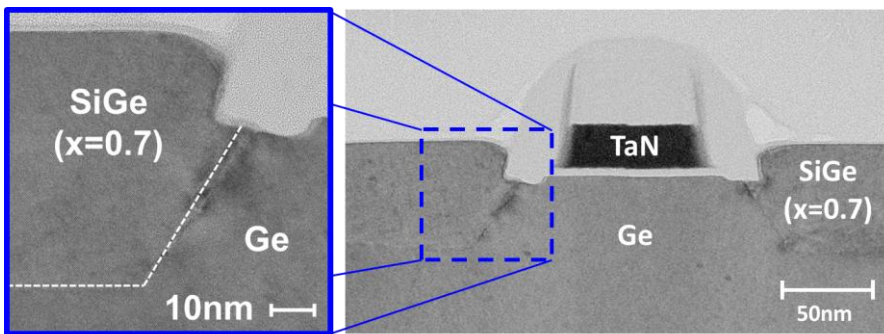


**Fig. 2** Cross-sectional TEM image of nMISFET with SiGe(x = 0.7) stressor.

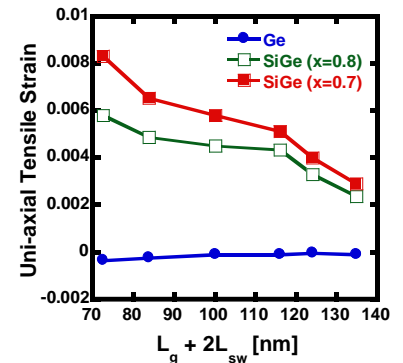


**Fig. 3** ( $L_g+2L_{sw}$ ) dependence of uniaxial tensile strain of Ge channel with SiGe stressor.

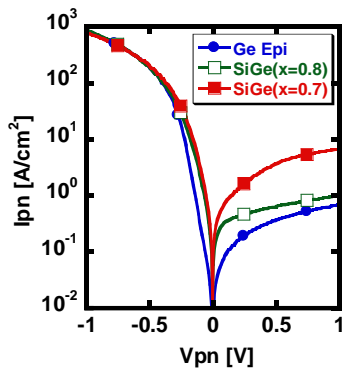


**Fig. 4** I-V curves for the n<sup>+</sup>Ge/pGe and n<sup>+</sup>SiGe/pSiGe diodes.

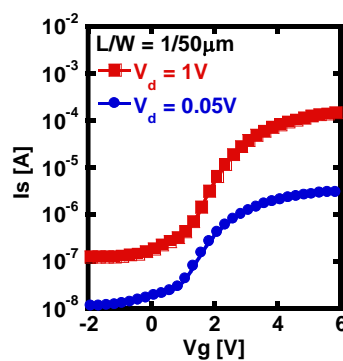


**Fig. 5**  $I_s$ - $V_g$  characteristics of  $L_g=1 \mu\text{m}$  nMISFET with SiGe(x = 0.7) stressor at  $V_d = 0.05 \text{ V}$  and  $1 \text{ V}$ .

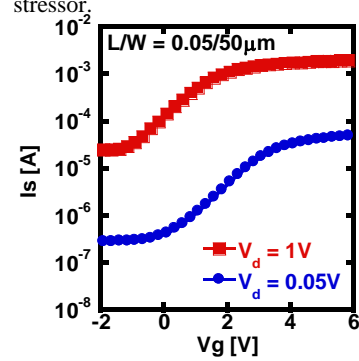


**Fig. 6**  $I_s$ - $V_g$  characteristics of  $L_g=50 \text{ nm}$  nMISFET with SiGe(x = 0.7) stressor at  $V_d = 0.05 \text{ V}$  and  $1 \text{ V}$ .

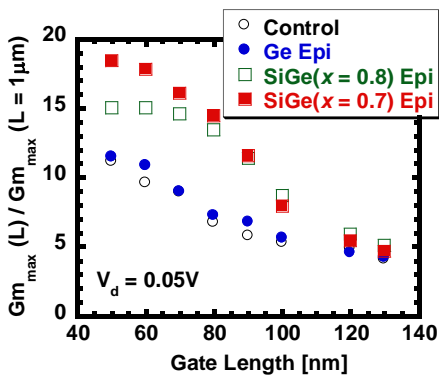


**Fig. 7** The normalized  $G_{m_{max}}$  as a function of  $L_g$  at  $V_d = 0.05 \text{ V}$ . The normalized  $G_{m_{max}}$  of SiGe(x = 0.8) and SiGe(x = 0.7) S/D device shows  $\sim 31\%$  and  $\sim 61\%$  gain over the control device at  $L_g = 50 \text{ nm}$ , respectively.

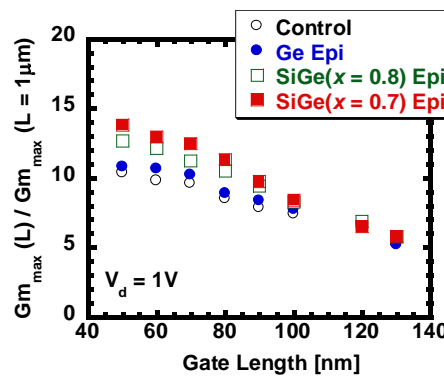


**Fig. 8** The normalized  $G_{m_{max}}$  as a function of  $L_g$  at  $V_d = 1 \text{ V}$ . The normalized  $G_{m_{max}}$  of SiGe(x = 0.8) and SiGe(x = 0.7) S/D device shows  $\sim 18\%$  and  $\sim 28\%$  gain over the control device at  $L_g = 50 \text{ nm}$ , respectively.

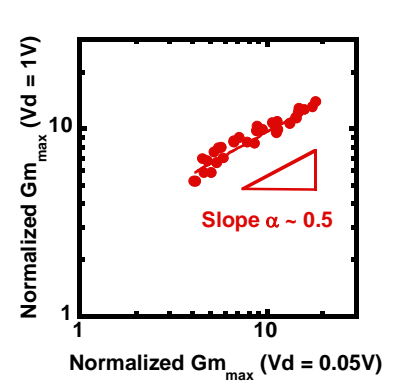


**Fig. 9** The Linear normalized  $G_{m_{max}}$  dependence of the saturation normalized  $G_{m_{max}}$ . The power of the linear normalized  $G_{m_{max}}$  dependence is about 0.5.